NANO · MICRO small
www.small-journal.com

Beyond Global Charge: Role of Amine Bulkiness and Protein Fingerprint on Nanoparticle–Cell Interaction

David Burnand, Ana Milosevic, Sandor Balog, Miguel Spuch-Calvar, Barbara Rothen-Rutishauser, Jörn Dengjel, Calum Kinnear, Thomas L. Moore,* and Alke Petri-Fink**

Amino groups presented on the surface of nanoparticles are well-known to be a predominant factor in the formation of the protein corona and subsequent cellular uptake. However, the molecular mechanism underpinning this relationship is poorly defined. This study investigates how amine type and density affect the protein corona and cellular association of gold nanoparticles with cells in vitro. Four specific poly(vinyl alcohol-*co*-*N*-vinylamine) copolymers are synthesized containing primary, secondary, or tertiary amines. Particle cellular association (i.e., cellular uptake and surface adsorption), as well as protein corona composition, are then investigated. It is found that the protein corona (as a consequence of "amine bulkiness") and amine density are both important in dictating cellular association. By evaluating the nanoparticle surface chemistry and the protein fingerprint, proteins that are significant in mediating particle–cell association are identified. In particular, primary amines, when exposed on the polymer side chain, are strongly correlated with the presence of alpha-2-HS-glycoprotein, and promote nanoparticle cellular association.

1. Introduction

Investigations into the interaction of nanoparticles (NPs) with biological systems have generally centered around the structure–function relationships between a NP's physicochemical properties and the effect of NPs on cells, or organisms. Biocompatible polymers are normally used to impart colloidal stability in biological media, attach targeting moieties, and increase circulation time following systemic administration. However, the chemical nature of these polymers affects the NPs' interaction with the biological environment by mediating the adsorption of proteins onto the NP surface, which influences cellular uptake. Many studies have investigated the role of NP size and shape toward cellular interaction.[1–3] Additionally, surface chemistry (e.g., surface charge) is known to strongly influence NP–cell association as well as the NP–protein interaction.[4,5] While the molecular mechanisms behind these observations are unclear, it is widely accepted that a net positive NP surface charge, mostly due to the presence of amino groups, is positively correlated with cellular uptake.[4–7] The greater cellular association of cationic NPs, compared to neutral or anionic ones, is generally explained as originating from Coulombic attraction of the NP to the negatively charged cell membrane. However, once NPs are incubated in cellular media, adsorbed serum proteins will dramatically alter the zeta (ζ) potential regardless of the initial inherent material surface charge.[4] Nevertheless, NPs coated with amino groups are still observed to associate stronger with cells in vitro. In one study, Townson et al.[8] compared the cellular uptake of NPs carrying amine groups either directly exposed to serum proteins or shielded by poly(ethylene glycol) (PEG). They concluded that the accessibility of the amino group to serum proteins correlates more strongly with cellular uptake than the measured surface charge. However, the role of the amine type (i.e., primary ($-NH_2$), secondary ($-NH(R)$), or tertiary ($-N(R)_2$)) is unclear, particularly as polyethylenimine (PEI) was used which carries a mixture of primary, secondary, and tertiary amines. In addition, the impact of the amine type, and accessibility, on the final protein corona is not known.

In a comprehensive study, Walkey et al.[9] investigated the impact of 105 different surface chemistries on the final NPs biological identity, that is, their protein corona and cellular association. They showed that the protein corona fingerprint

Dr. D. Burnand, Prof. A. Petri-Fink
Chemistry Department
Université de Fribourg
1700 Fribourg, Switzerland
E-mail: alke.fink@unifr.ch
Dr. D. Burnand, A. Milosevic, Dr. S. Balog, Dr. M. Spuch-Calvar, Prof. B. Rothen-Rutishauser, Dr. T. L. Moore, Prof. A. Petri-Fink
Adolphe Merkle Institute
Université de Fribourg
1700 Fribourg, Switzerland
E-mail: thomaslee.moore@unifr.ch
Prof. J. Dengjel
Department of Biology
Université de Fribourg
1700 Fribourg, Switzerland
Dr. C. Kinnear
School of Chemistry
University of Melbourne
Parkville 3010, Australia
E-mail: calum.kinnear@unimelb.edu.au
The ORCID identification number(s) for the author(s) of this article can be found under https://doi.org/10.1002/smll.201802088.

DOI: 10.1002/smll.201802088

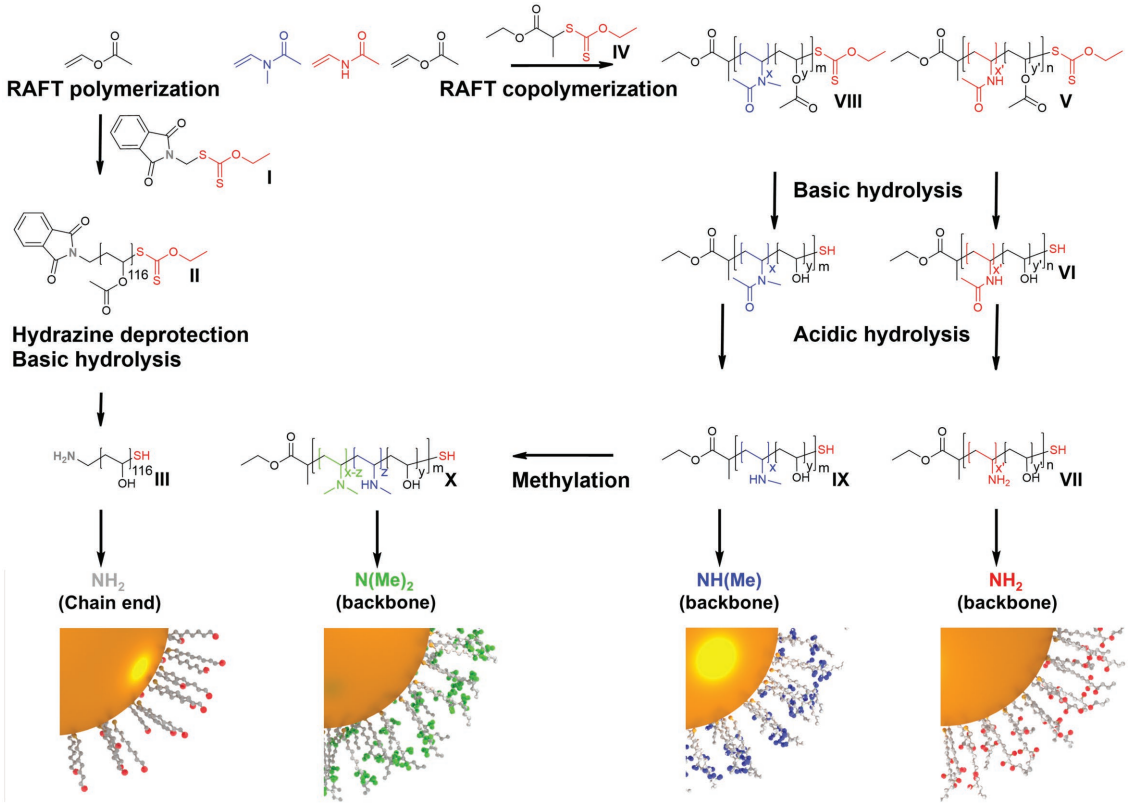

Figure 1. Schematic showing the polymers synthesis and the subsequent NPs functionalization.

could predict cellular association with 50% more accuracy than models considering the size, aggregation state, and surface charge. More recently, Treuel et al.[10] examined the literature and found that local surface charge variations, rather than the overall charge carried by the NP, better described the formed protein corona . However, there are few systematic studies investigating the nature of this relationship between molecularly induced surface charge and protein corona formation. It therefore remains challenging to determine what, if any, principal component is responsible for NP cellular uptake—that is, does amine type, density, or location (i.e., pendant vs chain end) dictate protein adsorption and particle uptake. Furthermore, can these interconnected effects be decoupled?[11]

In this work, we investigated the effect of amine type, density, and location on the cellular association of gold NPs with two cell lines, as well as the protein corona composition. To do this, four variations of poly(vinyl alcohol) (PVA) were synthesized with primary, secondary, or tertiary amino groups replacing the hydroxyl side chain groups, as well as one sample with a single terminal primary amino group (**Figure 1**). The polymers and NPs were extensively characterized both in simple and complex solvents via a range of techniques. While it was not possible to solely isolate amine type from amine density, our results provide evidence that supports the hypothesis that accessibility of amino groups (i.e., "amine bulkiness") is more important than average surface charge for both the composition of the protein corona and the resulting cellular association.

2. Results

2.1. Polymer Synthesis and Characterization

Taking inspiration from our previous work,[12,13] we used reversible addition-fragmentation chain transfer (RAFT) to copolymerize vinyl acetate, *N*-vinylacetamide, and *N*-methyl-vinylacetamide in order to obtain poly(vinyl acetate) with randomly placed primary (i.e., acetamide) and secondary (i.e., methyl acetamide) amine precursors, respectively (Figure 1).

Figure 2 shows ^{1}H NMR spectra for precursor species **V–VIII** and their final analogues **VII–X**. These data were used to determine polymer number-average molecular weight (M_n) as well as the amine content by integrating the methylene chain-end signal of the chain transfer agent (CTA) respective to the polymer backbone. Gel permeation chromatography (GPC) was used as a complementary method to verify the molecular weight distribution, as well as dispersity (Table S2, Supporting Information). Moreover, 2D ^{13}C-^{1}H NMR coupled with a colorimetric assay in which PVA forms a characteristic complex with a mixture of boric acid and KI/I_2 provided a means to measure the number of surface-bound amine groups.[14] **Table 1** shows the number of hydroxyl and amine groups on the polymer backbone, as well as the molecular weight after hydrolysis.

A fourth chemical entity (**III**) was also investigated using an *N*-terminal primary amine carried by the RAFT chain transfer agent.[15] This experiment was performed as a control in order to

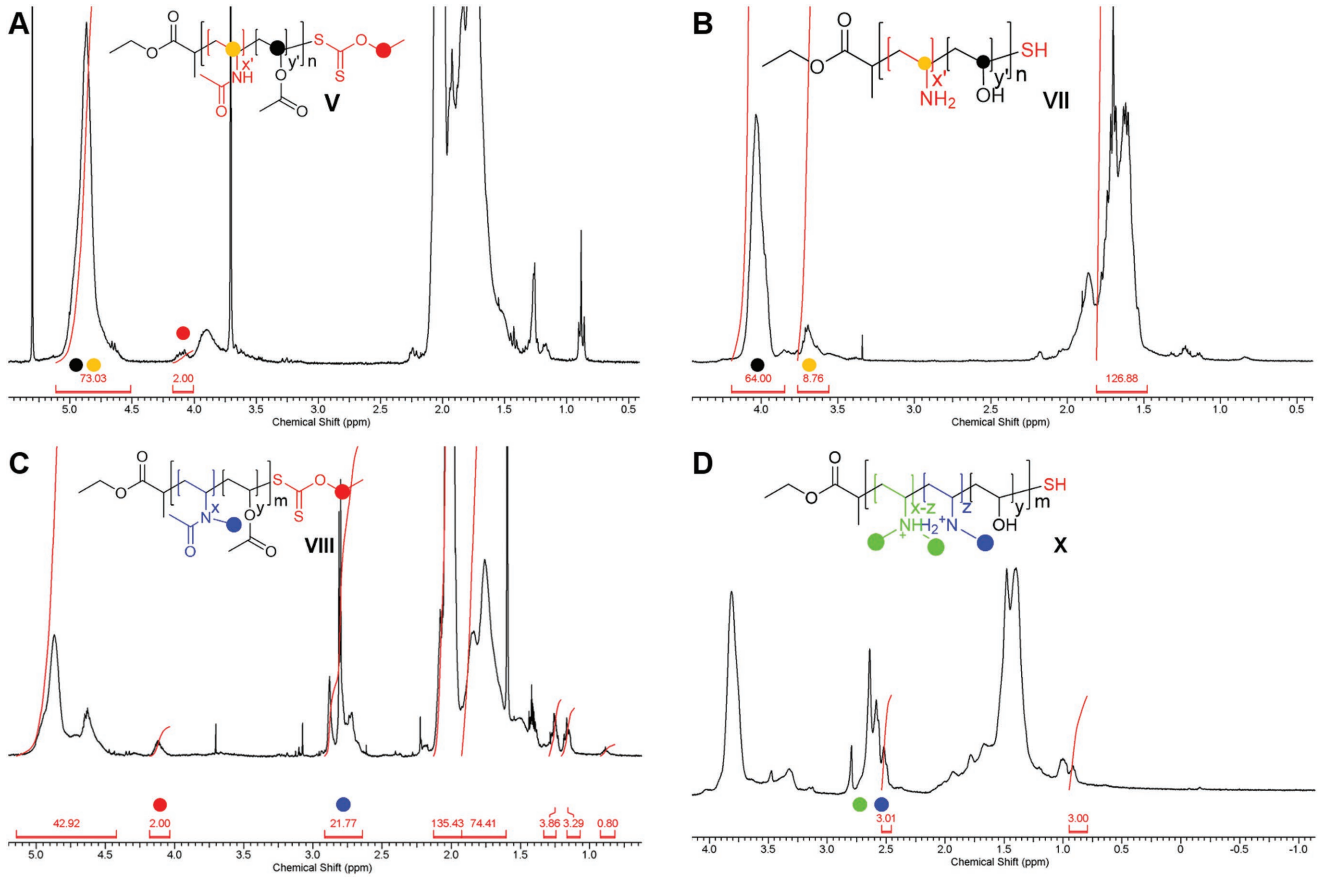

Figure 2. ^{1}H-NMR spectrum of A) poly(vinylacetate-*co*-*N*-vinylacetamide), **V**, B) hydrolyzed thiolated poly(vinyl alcohol-*co*-*N*-vinylamine), **VII**, C) poly(vinylacetate-*co*-*N*-methyl-vinylacetamide), **VII**, and D) hydrolyzed thiolated poly(vinyl alcohol-*co*-*N*-di-methyl-vinylamine), **X**. Signals used to calculate the molecular weight and the number of amines are illustrated, corresponding with the chemical structure shown.

test the location of the amine, that is, chain end versus side chain. The results of the polymer characterization are listed in Table 1.

Figure 3A,B shows the transmission electron microscopy (TEM) and size distribution of the gold NPs, with a core diameter of 26 ± 3 nm measured. Figure 3C and Figure S1 (Supporting Information) show the colloidal stability as assessed with UV–vis and depolarized dynamic light scattering (DDLS), and measured ζ-potential (**Table 2**) after 24 h exposure in RPMI media supplemented with 10% fetal bovine serum (FBS) at a concentration of 40 µg Au mL^{-1}. The UV–vis and DDLS data showed no characteristics of NP aggregation, and the characterization data are summarized in Table 2.

The polymer grafting density listed in Table 2 was assessed by characteristic colorimetric UV–vis complexometry of PVA with boric acid and KI/I_2. This enabled the calculation of the amine density given the known average number of amines per polymer chain as determined by NMR (Figure 2). Table 2 also lists the ζ-potential of the coated NPs in PBS, which ranged from neutral to negative depending on the adsorbed polymer. After incubation in supplemented media, all NPs were slightly negatively charged with magnitudes that can be considered similar given the complex scattering environment and lower accuracy of the measurement for ζ-potentials close to 0 mV. Additionally, the hydrodynamic diameters (d_H), measured via DDLS, were similar.

Table 1. Polymer coating characterization.

Polymer abbreviation	Coating polymers	−OH groups	Amine groups	M_n[a)] [Da]
Primary pendant	**VII**, NH_2 (backbone)	64	9	3300
Primary chain end	**III**, NH_2 (chain end)	116	1	5200
Secondary pendant	**IX**, NH(Me) (backbone)	36	7	2100
Tertiary pendant	**X**, $N(Me)_2$ (backbone)	36	6	2200

[a)]After hydrolysis.

2.2. Quantification of Cell-Associated NPs

A549 human lung epithelial and J774A.1 murine monocyte/macrophage cells lines were exposed to gold NPs with the four different surface chemistries and cellular association was measured using inductively coupled plasma-optical emission spectroscopy (ICP-OES). **Figure 4**A shows the number of NPs taken up per seeded A549 cell. Hereafter, for brevity, we consider the term uptake to refer to both endocytosed NPs and those adsorbed to the cell membrane. NPs coated with PVA with primary amines on the polymer backbone were significantly taken up compared to secondary or tertiary amines on the PVA backbone. Similar levels of cellular association were found for

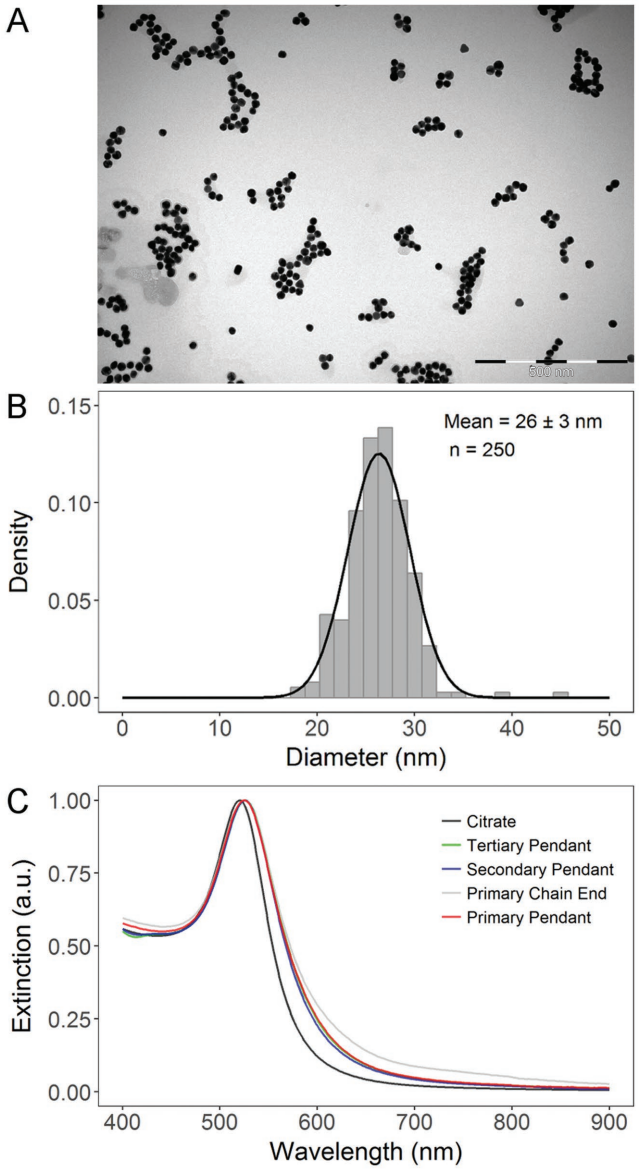

Figure 3. A) TEM image of citrate-gold NPs. B) Histogram showing Au NPs core diameter measured via TEM image analysis. Solid black line shows a normal density curve. C) UV–vis spectroscopy was utilized to evaluate NP colloidal stability after incubation for 24 h in RPMI-1640 cell culture media supplemented with 10% fetal bovine serum.

NPs coated with PVA bearing secondary or tertiary amino side groups.

NP cytotoxicity was evaluated with resazurin and lactate dehydrogenase assays to ensure NP-induced toxicity, or alterations in metabolic activity, did not influence the cellular uptake studies. As shown in Figure S2 (Supporting Information), we found that 40 μg Au mL^{-1} seemed to be at the upper viable concentration limit, as cell viability was at ≈85% for all particles coated with polymers bearing pendant amino groups for the J774A.1 cells (Figure S3, Supporting Information). This level of toxicity is likely due to the immense NP uptake and membrane disruption due to the high number of amino groups attached to the NP. For the A549 cells, only the pendant primary amino NPs showed significant toxicity which could again be attributed to the high level of cell uptake perturbing cellular function. In fact, only pendant primary amine NPs uptake by A549 cells was on the same order of magnitude as all pendant amine NPs uptake by J774A.1 cells.

2.3. Serum Protein Adsorption on Nanoparticle Surface

Cellular association is strongly dependent on the surface chemistry of the NP. However, the initial chemical identity provided by the different amine types evolves into a so-called biological identity upon adsorption of proteins. Figure 4C shows the relative amount (percentage) of four major proteins out of 240 measured that were adsorbed onto the different particle surfaces (172 without contamination from, e.g., keratins or uncharacterized proteins) after 24 h incubation in supplemented media. Proteins were separated using sodium dodecyl sulfate-polyacrylamide gel electrophoresis (SDS-PAGE) and identified by liquid chromatography tandem mass spectrometry (LC-MS/MS). We specifically investigated serum albumin, alpha-2-HS-glycoprotein, hemoglobin subunit alpha, and hemoglobin fetal subunit beta because the interparticle differences in protein adsorption between this cluster of proteins were greatest. Figure 4C shows that of these four major proteins, serum albumin and alpha-2-HS-glycoprotein were found to associate more with the NPs coated with primary amino groups than those coated by secondary or tertiary amines. The opposite trends can be seen for hemoglobin fetal subunit alpha and beta.

3. Discussion

3.1. Polymer Characterization

The RAFT copolymerization of vinyl acetate and *N*-vinyl amine derivatives is known to run with limited molecular weight control,[16] however, it can be used to synthesize polymers with thiolated end groups. These are ideal for grafting to the surface of gold NPs given the near-covalent strength of the gold–thiol bond.[17] Additionally, the variations in molecular weight between the amine-functionalized PVA polymers were very small compared with the typical size-dependent effects of cell penetration by cationic polymers.[18]

The molecular weights of the polymers determined by ^{1}H-NMR, as shown in Figure 2A,C, and by GPC, as shown in the Supporting Information, are in good agreement. For the determination by NMR, the ratio of the methylene signal of the ethyl ester located at the beginning of each polymer chain at 4.1 ppm and the signal of the repeat units at 4.9 ppm was used (Figure 2A,C **V**, **VIII**). Additionally, the number of amine groups for **VII** was determined by comparing the two backbone repeat unit signals at 4.0 and 3.6 ppm (Figure 2B **VII**).[19] Regarding **VIII**, the same methylene signal (4.1 ppm) was employed as a side chain reference and compared to the methyl signal of the protected secondary amine group at 2.8 ppm (Figure 2C **VIII**).

Matrix assisted laser desorption/ionization time of flight/mass spectrometry (MALDI-ToF/MS) was also used to verify the synthesis of copolymers **V** and **VIII** (Figure S5, Supporting Information). Both species were mono-isotopically resolved and fit with the calculated structures. Nevertheless, **V** required an aminolysis

Table 2. Nanoparticle characterization.

NPs	Amine density [amines nm^{-2}]	ζ-potential [mV ± SD]		d_H[b)] [nm ± SD]
		PBS[a)]	Supp. RPMI-1640[a)]	
Primary pendant	99	0 ± 5	−3 ± 7	45 ± 12
Primary chain end	4	−3 ± 1	−14 ± 7	54 ± 11
Secondary pendant	38	−29 ± 8	−14 ± 2	54 ± 14
Tertiary pendant	19	−30 ± 7	−9 ± 2	57 ± 14
Citrate	0	−45 ± 5	n.m.[c)]	25 ± 5[d)]

[a)]pH 7.3; [b)]Measured in complete RPMI-1640; [c)]Not measurable due to aggregation; [d)]Measured in Milli-Q water.

step to be detected and the oxidative form of the free end sulfur atom (i.e., sulfonate), most probably caused by the high laser power during the measurement itself, flew with sodium as a counterion. These two entities subsequently underwent a two-step hydrolysis (basic and acidic) to obtain the final free alcohol, as well as the desired amines. However, directly obtaining a tertiary amine is synthetically not possible. Therefore, the secondary amine copolymer (**IX**) was methylated using formaldehyde to form an iminium intermediate which was then reduced using a borane dimethylamine complex to obtain a tertiary amine **X**.[20–22]

3.2. Nanoparticle Characterization

Prior to adsorbing the polymers, the sodium-citrate coated gold NPs had a core diameter of 26 ± 3 nm as measured by TEM, 29 nm by UV–vis,[23] and a hydrodynamic diameter of 25 ± 5 nm as measured by intensity-weighted DDLS.[24] While traditionally the hydrodynamic diameter is greater than the core diameter measured via TEM, it is important to note that the particles here are uncoated with polymer and the excess sodium citrate in solution compresses the electrostatic double-layer to ≈1–2 nm, leading to an excellent agreement between the TEM and DDLS measurements within experimental error. The four end-thiolated polymers were then attached to the gold NPs by ligand exchange under basic conditions to avoid aggregation due to electrostatic interactions between the amino groups and the citrate molecules. The average quantity of adsorbed polymer was measured using a colorimetric PVA-complexation assay, combined with 2D ^{13}C-^{1}H NMR spectra, of the remaining PVA in the supernatant after separating the NPs via centrifugation (described further in the Supporting Information). This allowed us to define the average number of amines present on each NPs, expressed as an amine density.

After the NPs were coated with polymer and dispersed in PBS at pH 7.3, their ζ-potentials were measured. As expected for PVA-coated NPs, the ζ-potential ranged from neutral to negative depending on the adsorbed polymer.[12,25,26] We posit that there was no net positive charge due to the under representation of amino groups relative to hydroxyl groups on the chain backbone. Moreover, residual citrate could also be responsible for the negative ζ-potential values.

Upon incubation of the four NP samples for 24 h in supplemented cell culture media the ζ-potentials measured were similar, highlighting the charge shielding effect of protein adsorption. From the electrostatic argument outlined earlier, that is, that positive NPs interact stronger with negative cell membranes, all four samples are now similarly charged and should therefore be associated similarly with the cells in vitro. However, this is not the case as shown in Figure 4.

As outlined by various reports,[4,27,28] and recently highlighted as a major challenge for investigations of the NPs–cell interaction,[29] the aggregation, diffusion, and sedimentation of NPs in vitro are crucial parameters to ensure observations are reproducible. Here, we used DDLS to extract the hydrodynamic diameters, and thus assess the colloidal stability, of the coated gold NPs in cell culture media.[24] As shown in Figure 3A, the NPs are colloidally stable with only slight changes in their diameter as well as a slight redshift in the UV–vis spectra due to protein adsorption to the surface of the plasmonic NPs. However, the NPs coated with the primary chain end polymer had a slightly higher extinction in the range 650–900 nm. This could be due to the formation of a small number of dimers or trimers, however, the lack of any significant change in the hydrodynamic radius from DDLS indicates that the fraction of higher order structures is very small.

From the results described above, we assert that the four PVA-coated gold NPs samples possess very similar diameters, and therefore sedimentation and diffusion coefficients, as well as similar ζ-potentials. The relevant differences are then the quantity and type of polymer coating.

3.3. Nanoparticle–Cell Association

The A549 human lung epithelial and J774A.1 mouse monocyte macrophage cell lines were chosen for this study because they are frequently used as cell models to investigate NPs uptake, and to encourage comparisons with current literature.[30,31] Of these, the macrophages are known to be highly endocytotic with very rapid uptake of large quantities of nanomaterials and particle, sometimes even irrespective of small changes in particle size or shape.[3] This likely explains the similarity in measured uptake of the three polymer-functionalized NPs with pendant amino groups (Figure 4).

Contrary to the J774A.1 cells, A549 cells associated with NPs coated with secondary and tertiary amines far less than those coated with primary ones. Figure 4A shows that primary

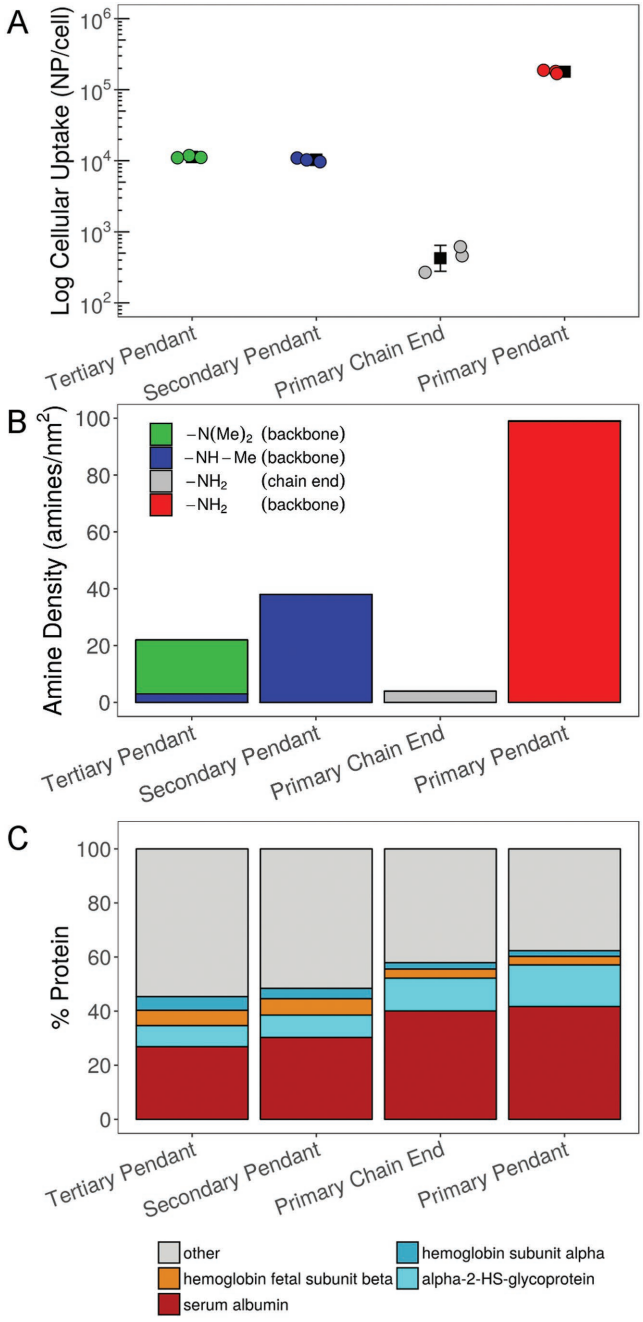

Figure 4. A) NP uptake by A549 human lung endothelial cells was measured by ICP-OES for the four different coatings. Uptake of pendant primary amino particles was an order of magnitude larger compared to secondary and tertiary pendant amino particles, and almost two orders of magnitude compared to the chain end primary amino. Black squares and error bars represent mean ± standard deviation. Filled circles represent individual replicates. B) Amine surface density for each NP formulation determined via 2D ^{13}C-^{1}H NMR coupled with UV–vis complexometry of PVA with boric acid and KI/I_2. C) Protein adsorption on the NP was determined via LC-MS/MS. Four relevant proteins were examined due to the significant changes in their adsorption amount—serum albumin, alpha-2-HS-glycoprotein, hemoglobin subunit alpha, and hemoglobin fetal subunit beta. Full protein adsorption characterization can be found in the Supporting Information.

amino groups increased the NP–cell association by around one order of magnitude. In addition, there was very little difference observed between the secondary and tertiary amino groups. We attribute these observations to the effective "bulkiness" of the amines, which includes their ability to form salt bridges, their hydrophobicity, and their effect on the conformation of the PVA coating, which alters the adsorbed protein corona. We discuss this in the following subsection.

There is one parameter which is not conserved across samples, and needs discussion, which is the relative amine density. As apparent from Table 2, the amine density is nonlinearly related to the cellular association. Given the known molecular weight-dependent, PEG-like "stealth" behavior of PVA, the sample with a single terminal primary amino group (which also has the highest molecular weight) likely behaves similarly to a stealth polymer coating resulting in very little interaction with the cells.[32,33] This may also be due to a greater chance of the single amino group being buried within the 116 hydroxyl-containing monomers.

The remaining three samples bearing pendant amino groups also differ in the calculated amine densities. However, the tertiary and primary amine densities in this study are 37 and 175 times above the saturation levels observed for aminated-dextran coated iron oxide NPs when incubated with T cells, that is, the amount of amine groups above which no greater increase in cell uptake was observed.[34] Therefore, this suggests that the observed differences in this study are more likely due to the type of amine, rather than the quantity, for those NPs coated with multiamine containing PVA. In addition, the ratio of amine to hydroxyl groups is nearly identical for all three samples. Nevertheless, further studies are needed to ascertain the validity and range of these assumptions, and we do not rule out the possibility that the different densities affect a secondary parameter, such as polymer conformation or internal hydrogen bonding within the PVA chains.

3.4. Nanoparticle–Protein Interactions

We investigated the total adsorption of proteins onto the different NPs via LC-MS/MS. Specifically, we focused on serum albumin, alpha-2-HS-glycoprotein, hemoglobin subunit alpha, and hemoglobin fetal subunit beta because this cluster of proteins is the most abundant on all the NPs' surface and was similarly highlighted by Clemments et al.,[35] who investigated the protein adsorption on alcohol (−OH) and primary amine ($-NH_2$) moieties on silica NPs. More closely related to our work, Sakulkhu et al.[36] probed the protein fingerprint of PVA/PVA−NH_2 and found a similar dominant protein cluster. Also, these four proteins were found to have the most dramatic difference in percent adsorption between the four polymer types. We found that the relative protein intensities changed according to the amine types, and this cluster of four proteins underwent significant changes in adsorption between NPs coated with tertiary/secondary or primary amines. Full LC-MS/MS protein adsorption data can be found in the Supporting Information.

Interestingly, protein adsorption was more closely related to the amino type, irrespective of amine density. For example, the

relative adsorption of serum albumin increases with primary amino groups which are either terminal or pendant. This result is striking because of the drastic difference in amine number and location on the polymer. The same trend was observed with alpha-2-HS-glycoprotein, where primary amino groups (terminal and pendant) led to an increase in adsorption compared to secondary or tertiary amino groups. Conversely, primary amino groups decreased the adsorption of hemoglobin fetal subunit beta and hemoglobin subunit alpha relative to the presence of secondary or tertiary amino groups. These findings are interesting because protein adsorption profiles are significant for determining the biological fate of NPs and it is apparent that amine bulkiness plays a role on the protein corona composition.

It was shown, by Walkey et al.,[9] that the ζ-potential predicted cellular association with more accuracy than models taking into account the total mass of adsorbed protein, the core diameter, the hydrodynamic diameter, or the local dielectric environment. The protein corona composition was more accurate again than the ζ-potential. However, we find that ζ-potential cannot explain the observed differences in cellular association—it is necessary to consider the protein composition. This leads us to postulate again that the amine "bulkiness" alters the adsorbed protein composition and thus determines the so-called "biological identity" of the NPs.

Regarding the types of proteins considered here, we hypothesize that serum albumin does not enhance NP uptake because it is the most abundant protein in blood and primarily functions as an osmotic regulator. Conversely, alpha-2-HS-glycoprotein is known to be involved in endocytosis and classified as an opsonin protein.[37–40] It is, however, important to note that one single protein does not mediate the observed trends in uptake. Rather, the cellular uptake of particles is a complex process related to particle physicochemical properties and the biological phenomena (i.e., protein corona composition, protein conformation, protein adsorption kinetics, particle–cell membrane interactions, etc.).

These data support our hypothesis that one and two bulky methyl groups inhibit the interaction between the amines and polar amino acids of serum proteins as speculated by Gessner et al.[41] In nature, the methylation of amino acids on histone tails (amine-rich nuclear proteins involved in the wrapping and packing of DNA) by *S*-adenosylmethionine inhibits the self-recognition mechanism responsible for the gene transcription.[42] To date there are few reported studies that have investigated the role of amine type on cellular uptake. Rather, large systematic studies have investigated multiple particle sizes, materials, surface functionalities (e.g., carboxylic acid, amine, alcohol), and cell types along with protein corona formation.

Lo et al.[43] investigated the cellular uptake of NPs made via the self-assembly of poly(2-(dimethylamino) ethyl methacrylate) (PDMAEMA), a polymer with side-chain tertiary amines, with DNA. Compared to DNA complexes made with linear polyethyleneimine (PEI), a polymer containing secondary amines in the polymer backbone, PDMAEMA/DNA NPs were more favorably taken up by BNL 1MEA.7R.1 murine liver cells. However, comparison between these studies in literature with our work is difficult due to the very nature of the particles compared: DNA polyplexes, where the amine is integral to DNA complexation, versus surface-modified NPs.

Previously, Sakulkhu et al.[44] identified proteins associated with the "hard corona" of superparamagnetic iron oxide NPs (SPIONs) coated with dextran or PVA, modified with positive, neutral, or negatively charged end groups. When comparing between PVA or dextran-coated NPs, apolipoprotein A-I and alpha-2-HS-glycoprotein were among the proteins identified to significantly adsorb onto PVA-coated NPs compared to dextran-coated NPs. A 2015 report by Ritz et al.[45] investigated the differences in protein corona formation and cellular uptake (human mesenchymal stem cells, hMSC) of polystyrene NPs with different surface functionalities. They showed a reduction in uptake of amine and sulfonate-functionalized NPs due to the enrichment of apolipoproteins on the NPs surface, and that apolipoprotein H was responsible for upregulating NPs uptake by hMSC. A study by Tenzer et al.[46] investigated the adsorption of proteins onto different silica or polystyrene particles. A number of serum proteins prominently adsorbed onto NPs irrespective of the surface functionality, for example, serum albumin, complement C3, apolipoprotein A-I, and Ig γ-1 chain C region. In these studies, we can learn that the adsorption of human serum protein is dependent on the serum type, particle surface, to an extent the time of exposure. Our report has specifically emphasized on the type of amines (i.e., the accessibility toward polar amino acids of serum proteins), and how this factor mediates protein corona formation and cellular uptake which has not been assessed before.

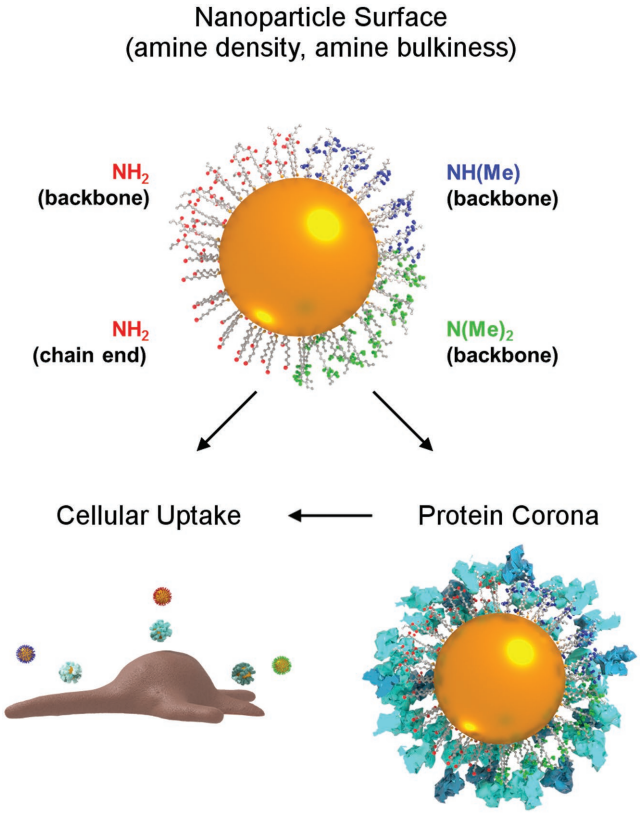

Figure 5. Schematic illustrating the three interconnected concepts: NP coated with primary, secondary, or tertiary amines, the protein corona formed on the particle surface in biological media, and the cellular uptake/association of NPs.

4. Conclusion

In this work we set out to elucidate how amine bulkiness, rather than global charge, could influence protein corona formation and subsequently particle-cell interaction (**Figure 5**). We have investigated the cellular association and protein corona of PVA-coated gold nanospheres with either primary, secondary, or tertiary amino groups added as PVA pendant groups, and found that methylation of the amines reduced the cellular association with A549 epithelial cells, although no differences were observed for J774A.1 macrophages. Little difference was found between secondary and tertiary amines in terms of cellular association or composition of the protein corona. We postulate that the effective "bulkiness" of the amines regulate binding of protein amino acids, causing changes in the adsorbed proteins and consequently the cellular association. While this indicates a potentially interesting and new way to modulate the interaction of aminated NPs with biological systems, further systematic studies are necessary to control for the amine density, polymer properties, and cell types. The robustness of the observed correlations should be assessed with respect to different biological environments (i.e., comparing protein coronas and endocytosis rates of NPs incubated in FBS supplemented media, human plasma, or whole blood) and different cell culture scales (i.e., cell lines in 2D or 3D cultures and primary cells).

Supporting Information

Supporting Information is available from the Wiley Online Library or from the author.

Acknowledgements

This project was supported by the Chemistry Department at the Université de Fribourg, the Adolphe Merkle Foundation, and the Swiss National Science Foundation through the National Center of Competence in Research Bio-Inspired Materials. C.K. acknowledges support from the Swiss National Science Foundation through an Early Postdoc.Mobility (P2FRP2_158730) and the ARC for support through CE170100026.

Conflict of Interest

The authors declare no conflict of interest.

Keywords

amine density, nanoparticle, particle–cell interaction, protein fingerprint, surface charge

Received: May 31, 2018
Revised: July 11, 2018
Published online: September 10, 2018

[1] L. Shang, K. Nienhaus, G. U. Nienhaus, *J. Nanobiotechnol.* **2014**, *12*, 5.
[2] Z. Mao, X. Zhou, C. Gao, *Biomater. Sci.* **2013**, *1*, 896.
[3] C. Kinnear, T. L. Moore, L. Rodriguez-Lorenzo, B. Rothen-Rutishauser, A. Petri-Fink, *Chem. Rev.* **2017**, *117*, 11476.
[4] V. Hirsch, C. Kinnear, M. Moniatte, B. Rothen-Rutishauser, M. J. D. Clift, A. Fink, *Nanoscale* **2013**, *5*, 3723.
[5] A. Verma, F. Stellacci, *Small* **2010**, *6*, 12.
[6] K. Fytianos, L. Rodriguez-Lorenzo, M. J. D. Clift, F. Blank, D. Vanhecke, C. Von Garnier, A. Petri-Fink, B. Rothen-Rutishauser, *Nanomed.: Nanotechnol., Biol. Med.* **2015**, *11*, 633.
[7] Y. Yuan, C. Mao, X. Du, J. Du, F. Wang, J. Wang, *Adv. Mater.* **2012**, *24*, 5476.
[8] J. L. Townson, Y.-S. Lin, J. O. Agola, E. C. Carnes, H. S. Leong, J. D. Lewis, C. L. Haynes, C. J. Brinker, *J. Am. Chem. Soc.* **2013**, *135*, 16030.
[9] C. D. Walkey, J. B. Olsen, F. Song, R. Liu, H. Guo, D. W. H. Olsen, Y. Cohen, A. Emili, W. C. W. Chan, *ACS Nano* **2014**, *8*, 2439.
[10] L. Treuel, D. Docter, M. Maskos, R. H. Stauber, *Beilstein J. Nanotechnol.* **2015**, *6*, 857.
[11] P. Rivera-Gil, D. Jimenez De Aberasturi, V. Wulf, B. Pelaz, P. Del Pino, Y. Zhao, J. M. De La Fuente, I. Ruiz De Larramendi, T. Rojo, X.-J. Liang, *Acc. Chem. Res.* **2013**, *46*, 743.
[12] C. Kinnear, D. Burnand, M. J. D. Clift, A. F. M. Kilbinger, B. Rothen-Rutishauser, A. Petri-Fink, *Angew. Chem., Int. Ed.* **2014**, *53*, 12613.
[13] D. Burnand, C. A. Monnier, A. Redjem, M. Schaefer, B. Rothen-Rutishauser, A. Kilbinger, A. Petri-Fink, *J. Magn. Magn. Mater.* **2015**, *380*, 157.
[14] D. P. Joshi, Y. L. Lan-Chun-Fung, J. G. Pritchard, *Anal. Chim. Acta* **1979**, *104*, 153.
[15] A. A. A. Smith, T. Hussmann, J. Elich, A. Postma, M.-H. Alves, A. N. Zelikin, *Polym. Chem.* **2012**, *3*, 85.
[16] K. Nakabayashi, H. Mori, *Eur. Polym. J.* **2013**, *49*, 2808.
[17] R. A. Sperling, W. J. Parak, *Philos. Trans. R. Soc., A* **2010**, *368*, 1333.
[18] M. Hellmund, K. Achazi, F. Neumann, B. N. S. Thota, N. Ma, R. Haag, *Biomater. Sci.* **2015**, *3*, 1459.
[19] M. Dréan, P. Guégan, C. Jérôme, J. Rieger, A. Debuigne, *Polym. Chem.* **2016**, *7*, 69.
[20] G. E. Means, R. E. Feeney, *Biochemistry* **1968**, *7*, 2192.
[21] W. R. Rypniewski, H. M. Holden, I. Rayment, *Biochemistry* **1993**, *32*, 9851.
[22] Y. Kim, P. Quartey, H. Li, L. Volkart, C. Hatzos, C. Chang, B. Nocek, M. Cuff, J. Osipiuk, K. Tan, *Nat. Methods* **2008**, *5*, 853.
[23] W. Haiss, N. T. K. Thanh, J. Aveyard, D. G. Fernig, *Anal. Chem.* **2007**, *79*, 4215.
[24] S. Balog, L. Rodriguez-Lorenzo, C. A. Monnier, M. Obiols-Rabasa, B. Rothen-Rutishauser, P. Schurtenberger, A. Petri-Fink, *Nanoscale* **2015**, *7*, 5991.
[25] R. Kurchania, S. S. Sawant, R. J. Ball, *J. Am. Ceram. Soc.* **2014**, *97*, 3208.
[26] F. A. Sheikh, N. A. M. Barakat, M. A. Kanjwal, S. J. Park, D. K. Park, H. Y. Kim, *Macromol. Res.* **2010**, *18*, 59.
[27] A. Albanese, W. C. W. Chan, *ACS Nano* **2011**, *5*, 5478.
[28] T. L. Moore, L. Rodriguez-Lorenzo, V. Hirsch, S. Balog, D. Urban, C. Jud, B. Rothen-Rutishauser, M. Lattuada, A. Petri-Fink, *Chem. Soc. Rev.* **2015**, *44*, 6287.
[29] M. Henriksen-Lacey, S. Carregal-Romero, L. M. Liz-Marzán, *Bioconjugate Chem.* **2017**, *28*, 212.
[30] R. Zhu, Q. Wang, Y. Zhu, Z. Wang, H. Zhang, B. Wu, X. Wu, S. Wang, *Acta Biomater.* **2016**, *29*, 320.
[31] A. Semisch, J. Ohle, B. Witt, A. Hartwig, *Part. Fibre Toxicol.* **2014**, *11*, 10.
[32] H. Takeuchi, H. Kojima, H. Yamamoto, Y. Kawashima, *J. Controlled Release* **2001**, *75*, 83.
[33] B. M. Budhlall, K. Landfester, E. D. Sudol, V. L. Dimonie, A. Klein, M. S. El-Aasser, *Macromolecules* **2003**, *36*, 9477.
[34] D. L. J. Thorek, A. Tsourkas, *Biomaterials* **2008**, *29*, 3583.
[35] A. M. Clemments, C. Muniesa, C. C. Landry, P. Botella, *RSC Adv.* **2014**, *4*, 29134.
[36] U. Sakulkhu, M. Mahmoudi, L. Maurizi, G. Coullerez, M. Hofmann-Amtenbrink, M. Vries, M. Motazacker, F. Rezaee, H. Hofmann, *Biomater. Sci.* **2015**, *3*, 265.

[37] P. Arnaud, L. Kalabay, *Diabetes/Metab. Res. Rev.* **2002**, *18*, 311.
[38] H. Jersmann, K. A. Ross, S. Vivers, S. B. Brown, C. Haslett, I. Dransfield, *Cytometry* **2003**, *51A*, 7.
[39] S. Nagayama, K. Ogawara, K. Minato, Y. Fukuoka, Y. Takakura, M. Hashida, K. Higaki, T. Kimura, *Int. J. Pharm.* **2007**, *329*, 192.
[40] A. M. Sakwe, R. Koumangoye, S. J. Goodwin, J. Ochieng, *J. Biol. Chem.* **2010**, *285*, 41827.
[41] A. Gessner, R. Waicz, A. Lieske, B.-R. Paulke, K. Mäder, R. H. Müller, *Int. J. Pharm.* **2000**, *196*, 245.
[42] S. C. Lu, *Int. J. Biochem. Cell Biol.* **2000**, *32*, 391.
[43] C.-W. Lo, Y. Chang, J.-L. Lee, W.-B. Tsai, W.-S. Chen, *PLoS One* **2014**, *9*, e97627.
[44] U. Sakulkhu, M. Mahmoudi, L. Maurizi, J. Salaklang, H. Hofmann, *Sci. Rep.* **2015**, *4*, 5020.
[45] S. Ritz, S. Schöttler, N. Kotman, G. Baier, A. Musyanovych, J. Kuharev, K. Landfester, H. Schild, O. Jahn, S. Tenzer, *Biomacromolecules* **2015**, *16*, 1311.
[46] S. Tenzer, D. Docter, J. Kuharev, A. Musyanovych, V. Fetz, R. Hecht, F. Schlenk, D. Fischer, K. Kiouptsi, C. Reinhardt, *Nat. Nanotechnol.* **2013**, *8*, 772.